

INFLUENCE OF THE LAYER THICKNESS ON THE VERY HIGH CYCLE FATIGUE BEHAVIOUR OF COMPOSITE MATERIALS

Martin Bartelt¹, Tim Luplow¹, Peter Horst¹, Sebastian Heimbs¹

¹ TU Braunschweig, Institute of Aircraft Design and Lightweight Structures (IFL),
Hermann-Blenk-Str. 35, 38108 Braunschweig, Germany
martin.bartelt@tu-braunschweig.de

Abstract: High-efficiency structures like blades of wind turbines and helicopters undergo over 10^8 load cycles during their lifetime. For fibre-reinforced composite materials, a lack of research in this so-called region of very high cycle fatigue may lead to conservative designs or fatal failures. One aspect known for its strong influence on static and fatigue crack initiation is the layer thickness of the composite plies. Thin layers promise higher lifetimes and enhanced structures.

To investigate this effect, the two cross-ply lay-ups $(90_2/0_2)_s$ and $(90/0)_{2s}$ with 0.5 mm and 0.25 mm layer thickness, respectively, are tested in a specialised very high cycle fatigue four-point bending test system. The composite material consists of the fatigue-optimised fibre SE2020 from 3B-fibreglas and the epoxy resin system RIM135. Transmitted light photography is used to determine the two important fatigue damage parameters crack density and delamination area ratio. Also, general damage mechanisms and the flexural modulus degradation are assessed to identify the influence of the ply thickness.

Comparing the photographs of the test series, a higher crack density is immediately noticeable for the thin layers. Quantitative data determined from the photographs by a specially developed damage detection software confirms this and shows larger delaminations per crack for thicker layers.

With a finite element model, the influence of the crack density and delamination area ratio on the damage development is investigated. Plotting the surface strain and the stress intensity factor over the damage parameters, the influence of the ply thickness is directly visible and the development of a “damage path” and different ratios between the damage parameters can be understood.

Keywords: VHCF, Ply thickness, Cross-ply, Transverse cracking, Delamination

1. INTRODUCTION

The fatigue of fibre-reinforced plastics (FRP) is a wide field being researched since the 1960s. The growing use of FRP in high-performance and -efficiency structures, some also with high safety relevance, drives the motivation to understand the complex fatigue behaviour. A special branch of research is the very high cycle fatigue (VHCF) with up to 10^8 load cycles (LC), which applies to rotor blades of helicopters and wind turbines as well as aircraft propellers [1, 2]. Due to long testing times (386 days for 10^8 LC at 3 Hz), specimen heating under high test frequencies, self-fatigue of the test

equipment and other issues the research of the VHCF behaviour is scarce [3]. A lot of the existing work concentrates on total failure plotted as SN-curves, failure prediction and fatigue limits. Missing knowledge is compensated by a conservative (and ineffective) design. An overview of test methods and damage mechanisms is given by Shabani et al. [4].

This paper treats the influence of the layer thickness under consideration of damage parameters. This is the second part of a research series covering the influences of materials [5], layer thickness, stress ratio and loading type under VHCF using cross-ply laminates.

Thinner layers are known for higher strength and crack initiation stresses under quasi-static loading [6, 7, 8]. This is explained by smaller initial flaws or a limitation effect from adjacent layers. The investigations from Hannig [9] show that this behaviour is not transferable to fatigue loading up to 10^5 LC.

More general findings from Boniface, Ogin, Smith and Bader [10, 11, 12, 13] show a similar increase of transverse crack density with decreasing layer thickness for quasi-static and fatigue loading. Also, they find a slower crack growth in thin layers and a dependence of crack growth from crack spacing.

The damage mechanisms of quasi-isotropic and cross-ply CFRP laminates under tensile loading are investigated by Hosoi et al. [14, 15] up to 10^8 LC. They determine important fatigue damage parameters like the transverse crack density and the delamination area ratio. They identify later crack initiation and higher crack densities for thin layers and larger delaminations for thick layers.

Fundamental work for the investigations presented here was conducted by Adam and Horst [16, 17, 18, 19]. This contains the development of a four-point bending VHCF test rig and test series on angle- and cross-ply GFRP laminates. They found typical fatigue damages under bending up to 10^8 LC as they are already known for tension like transverse cracking in the 90° -layer and delaminations on the interface to the adjacent 0° -layer.

To determine the influence of the layer thickness under four-point bending in the VHCF region, the experimental approach containing materials and specimens, the specialised test system, the conducted test series and the damage evaluation parameters is explained first. Then, the numerical simulation model is introduced. The evaluations start with an overview of the fatigue damages for the four test series (TS) and all load levels (LL) and continue with the quantitative damage parameters. Finally, the identified effects are investigated via a parametric simulation of relevant crack densities and delamination area ratios.

2. EXPERIMENTAL APPROACH

The composite material used for the specimens of the four TS in this study consists of a glass fibre / epoxy system. All TS are conducted in a specialised VHCF four-point bending test rig under the same experimental parameters, except of the layer thickness and the stress ratio. For damage evaluation the flexural modulus is recorded by the test system and photographs are taken automatically during the fatigue test. A damage detection software identifies the crack density and delamination area ratio for every photograph.

2.1 Material and Specimens

For the FRP the glass fibre *SE2020* from *3B fibreglass* is combined with the epoxy resin system *RIM135R / RIM137H* from *Hexion*. According to the manufacturers brochure the fibre is optimised for fatigue by a special sizing. This results in an enhanced fibre-matrix adhesion like it is shown by Bartelt et al. [5] in comparison with another fibre and the same matrix material. The resulting improved crack resistance leads to higher lifetimes and shifts the fatigue damages from cracking to more delaminations. The manufacturing process starts with CNC-roving stacking for unsewn laminates, which enables investigation of a laminate with less disturbance (due to the missing sewing threads). The fabric is then infiltrated with the epoxy resin using the resin transfer moulding process. This process yields high

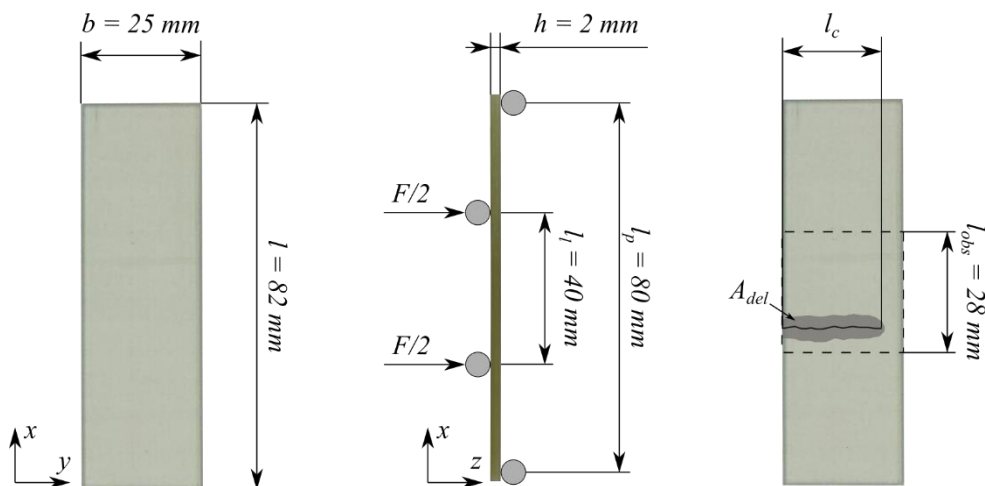


Figure 1: Geometric parameters of the specimens, four-point bending device and damage evaluation.

quality laminates with smooth surfaces and high transparency. In the next step the specimens are cut out by CNC-milling to guarantee the correct laminate angle. Then the specimen edges are ground and polished to prevent additional crack initiation due to prior damages. The geometric parameters of the specimens are shown in Figure 1 and the mechanical properties of the unidirectional (UD) laminate are listed in Table 1.

Table 1: Tensile mechanical properties of the UD-laminates as characterised by Chen [20].

Mech. Properties	Unit	SE2020 / RIM135
E_{11}	GPa	33.8
E_{22}	GPa	7.8
R_{11}	MPa	744
R_{22}	MPa	60
ϵ_{11}	%	2.33
ϵ_{22}	%	1.1
ϕ_f	%	39.7

To investigate the layer thickness the two cross-ply lay-ups $(90_2/0_2)_s$ and $(90/0)_{2s}$ are manufactured. One layer of the 600 tex roving yields a layer thickness of 0.25 mm. By stacking two layers with the same direction on top of another, a thickness of 0.5 mm is reached. These stacked layers are not distinguishable under the microscope. Microscopic photographs of both lay-ups are shown in Figure 2. The influence of the layer thickness can be determined with less disturbances, because damage interactions are fewer in cross-ply laminates compared to quasi-isotropic laminates.

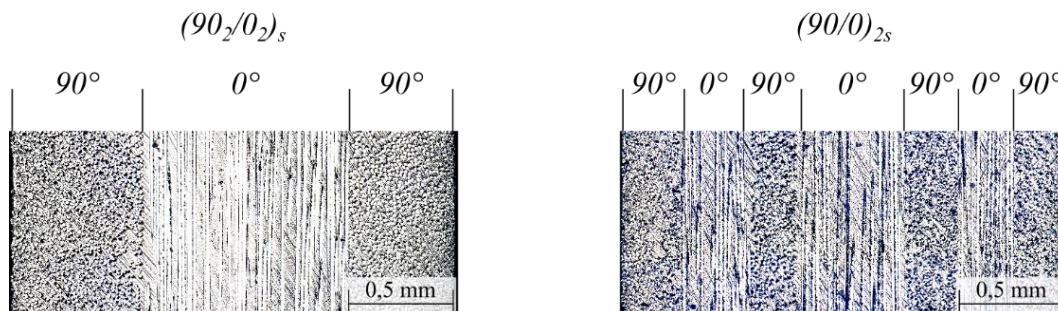


Figure 2: Microscopic photograph of the side of two specimens revealing the two lay-ups.

2.2 VHCF Four-Point Bending Test System

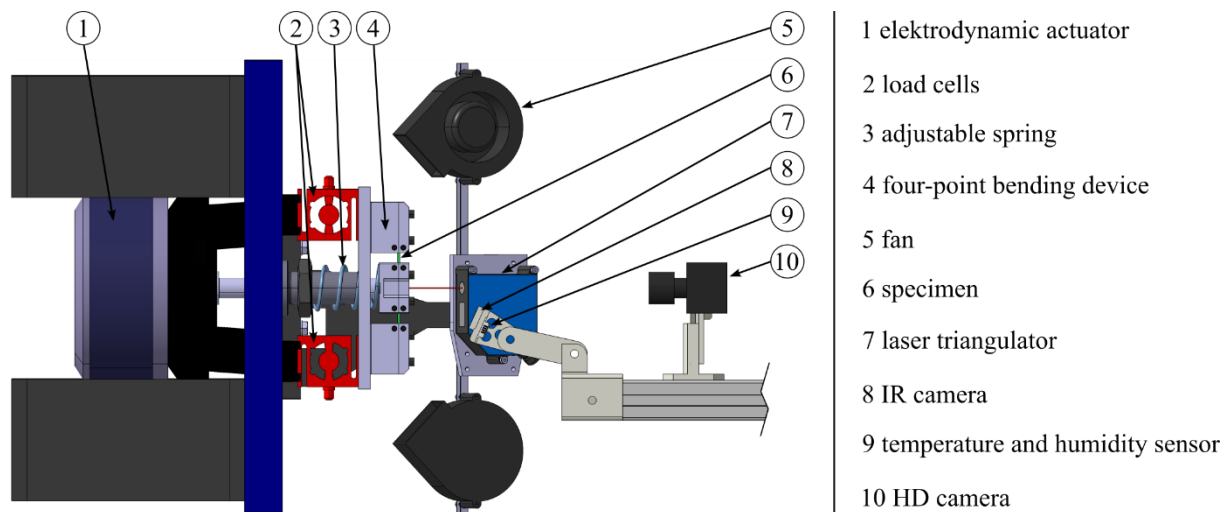


Figure 3: One of four test units of the VHCF test system.

Fatigue testing up to 10^8 load cycles requires a specialised test rig to overcome problems like long testing times, self-fatigue of the test rig and specimen heating. Therefore, Adam and Horst [16] developed the VHCF four-point bending test system shown in Figure 3 that addresses these problems. To conduct this study, the test rig is upgraded regarding an improved measurement accuracy and several new features. Four-point bending acquires lower forces at larger deflections compared to tensile loading. This allows the use of an electrodynamic actuator, solving the problem of self-fatigue of the mostly used hydraulic or mechanical actuators. The actuator deflects the inner bearing of the four-point bending device with frequencies from 20 Hz to 80 Hz. The specimen is mounted between the two outer bearings and is deflected by the inner bearing. The geometry of the bending device is given in Figure 1. The applied load is measured by two load cells mounted on the same base plate like the actuator. A laser triangulator measures the centre deflection of the specimen.

During upgrading of the test system, the external photo camera and infrared (IR) camera were replaced by devices connected to the control system. This allows automatic recording of photographs and temperature data, as well as automated control of the two cooling fans.

To enable testing with variable stress ratios an adjustable spring is added to apply a constant load onto the inner bearing. Also, the control software (*NI LabVIEW*) is updated to record and retain the stress ratio by adding a direct current to the alternating load signal.

The described test unit is one of four units mounted on a damping concrete base. The entire test system is placed inside a thermal and sound insulating housing. An air-condition keeps the ambient temperature at 20°C.

2.3 Conducted Experiments

For this study, four test series with varying layer thickness and stress ratio are conducted, evaluated and compared. The testing parameters are listed in Table 2. To determine the influence of the layer thickness, comparison takes place between TS1 and TS2 under a stress ratio of $R = -1$ and between TS3 and TS4 under $R = 0.1$. The influence of the stress ratio is not discussed here and will be investigated in a separate study.

For every TS multiple specimens are tested on one of up to seven load levels. The load levels are defined by the surface strain of the outer 90°-layer at the beginning of the fatigue test $\epsilon_{22,0}^{90^\circ}$ and are listed with the number of specimens for every TS in Table 3.

Table 2: Fatigue testing parameters of the four test series.

Test Series	Lay-up	Layer Thickness	Stress Ratio
		t_{90}	R
1	(90 ₂ /0 ₂) _s	0.5	-1
2	(90/0) _{2s}	0.25	-1
3	(90 ₂ /0 ₂) _s	0.5	0.1
4	(90/0) _{2s}	0.25	0.1

Table 3: Number of specimens tested per load level and test series.

Load level	Surface strain	Number of specimens			
	$\varepsilon_{22,0}^{90^\circ}$	TS1	TS2	TS3	TS4
1	0.68	2	3	4	4
2	0.55	2	2	4	4
3	0.43	4	3	4	4
4	0.36	4	5	4	4
5	0.30	4	5		
6	0.25	4	4		
7	0.22	3			
	Total	23	22	16	16

Every specimen is tested up to 10^8 load cycles or until very high damage states are reached and no more damage development can be expected. These high damage states indicate that the load level belongs more to the region of high cycle fatigue (HCF, up to 10^6 LC), than to VHCF. This is the case for LL1 and LL2 of TS1 and TS2. These load levels are still useful to compare the phenomena and to relate them to the VHCF results.

The test frequency is chosen close to the natural frequency of the specimen and test system (50 Hz to 55 Hz). At this frequency the test duration for one specimen is about four weeks.

For verification of the test results, the flexural modulus of every specimen is measured before and after the fatigue test on a quasi-static four-point bending test stand.

2.4 Damage Evaluation

For cross-ply laminates under bending the typical fatigue damages are transverse cracks in the outer 90°-layers and delaminations growing from the crack tip along the interface to the adjacent 0°-layer. With growing damages, the mechanical properties of the material degrade. This leads to the evaluation of the fatigue damages by the three parameters degradation of the outer 90°-layer under tension $D_{x,b}^{90^\circ}$, crack density ρ and delamination area ratio H_{del} .

Compared to three-point bending, four-point bending provides a large observation area under a constant bending moment shown in Figure 1 (right). The high transparency of the laminate enables damage detection through transmitted light photography. Therefore, a white LED-screen is mounted between the inner bearings of the bending device behind the specimen (Figure 3). The damage parameters are calculated similar to Adam et al. [17].

To calculate the degradation of the outer 90°-layer, the flexural modulus measured by the test system and the ply discount value are needed.

The equation of the simplified flexural modulus under four-point bending is

$$\bar{E}_{x,b} = \frac{\hat{F}}{\hat{w}_{max}} \frac{(l_P - l_L)}{bh^3} \left(\frac{1}{4}(l_P - l_L)^2 + \frac{3}{4}l_L(l_P - l_L) + \frac{3}{8}l_L^2 \right), \quad (1)$$

with the force and deflection amplitudes \hat{F} and \hat{w}_{max} . Variables b and h are the specimen width and thickness. The inner and outer bearing distances are designated as l_L and l_p .

The ply discount value represents the flexural modulus of the laminate without the 90°-layer under tension and is calculated using the classical laminate theory. For the (90₂/0₂)_s-lay-up it is about 64.1 % of the flexural modulus before the fatigue test $E_{x,b,0}$ and 82.9 % for the (90/0)_{2s}-lay-up.

For a certain load cycle n the degradation of the outer 90°-layer is defined by:

$$D_{x,b,n}^{90^\circ} = \frac{E_{x,b,n} - E_{x,b,PDV}}{E_{x,b,0} - E_{x,b,PDV}}. \quad (2)$$

To calculate the crack density

$$\rho = \frac{\sum_{i=0}^{n_c} l_{c,i}}{b_{obs} l_{obs}} \quad (3)$$

the sum of all crack lengths $l_{c,i}$ is divided by the observation area $b_{obs} \cdot l_{obs}$.

With the delamination area A_{del} the delamination area ratio

$$H_{del} = \frac{A_{del}}{b_{obs} l_{obs}} \quad (4)$$

is calculated similarly. The parameters l_c and A_{del} are shown in Figure 1. For test series with cracks and delaminations on the front- and back-side (only for $R = -1$), all crack lengths and delamination areas are added and divided by twice the observation area.

Due to the automation of the specimen photography, the number of pictures per fatigue test rises from around ten manually to 100 automatically taken pictures. With the advantage of a higher density of data points comes the disadvantage of much more evaluation work. This disadvantage is encountered with the development of an automated crack- and delamination detection software, using *Python* and the *OpenCV* library. By comparison to manual measured data the software is successfully validated.

For high damage states, like they occur under HCF, the chance of a front side crack or delamination covering the same damage on the back side rises. A covered back side damage cannot be distinguished on a photography manually or by the detection software. This means, the method of damage detection through transmitted light photography is only valid for low damage accumulations, as they typically occur under VHCF.

3. PARAMETRIC CRACK AND DELAMINATION SIMULATION MODEL

From the experimental results, several phenomena can be observed and may be related to the influence of the layer thickness. To support the understanding of these phenomena and the impact of the layer thickness, the parametric fatigue damage simulation model, shown in Figure 4, is developed using *ANSYS* and its parametric design language *APDL*. Parametric inputs are:

- the loading type (four-point bending / tension)
- the lay-up and material parameters
- the x-position of a variable number of cracks in the outer layer
- the length of delaminations at the crack tip along the layer interface

Beside the displacement and the stress distribution, the stress intensity factors (SIF) are calculated at the crack tip. Solid 186 and Solid 187 elements are used to enable the calculation of the SIF. The results are verified with analytical solutions. Also, the reduction of the specimen width from 25 mm to 4 mm, to reduce calculation time, is checked not to lead to significant differences in the results.

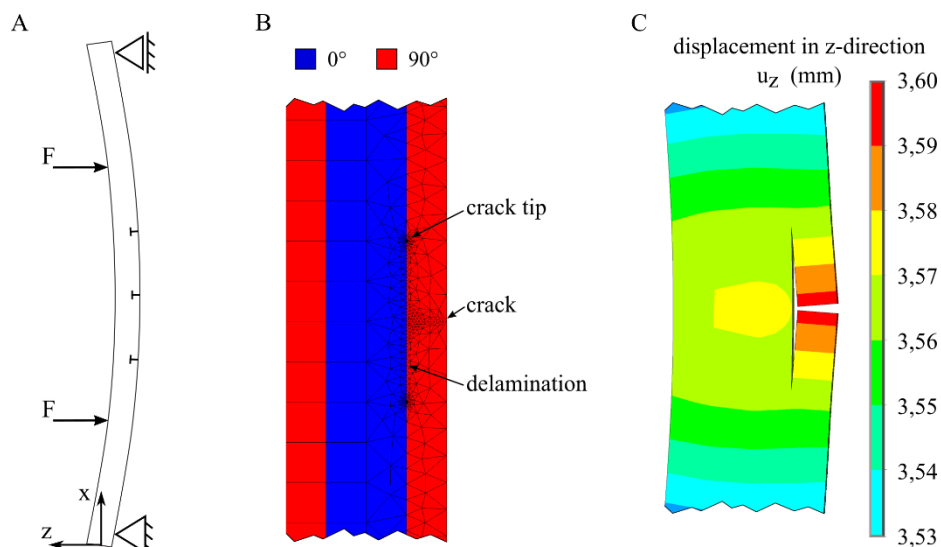


Figure 4: Numerical model overview: (A) Three cracks with delaminations simulated on the full specimen model, (B) close-up view of refined mesh and the lay-up at the centre crack, (C) displacement at the centre crack under LL3, according to Bartelt et al. [5].

4. INFLUENCE OF THE LAYER THICKNESS

Looking at the linear increasing strain over the laminate thickness under bending, the mean strain of the 0.25 mm layer is higher, with 87.5 % of the surface strain, than the mean strain of the 0.5 mm layer with 75 % of the surface strain. As the maximum strain is considered to be very important under VHCF, the load levels refer to the surface strain. Nevertheless, the difference of mean layer strain should be kept in mind for the following evaluations.

These begin with the photographic overview of the fatigue test series and continue with the quantitative damage parameters. Finally, numerical investigations on the crack density and delamination area ratio follow.

4.1 Fatigue Results Overview

An overview of the fatigue damages for all test series with one characteristic specimen per load level is given in Figure 5. The range of damages reaches from damage-free specimens to highly damaged ones for every test series, pointing out the correct choice of load levels. As to be expected, the damages increase with the load levels, indicating a valid fatigue testing. Also, the consistency of the fatigue damage of the specimens within the load levels is strong (not shown here). Uneven crack spacing is considered as weak spot cracking (low loads), whereas equal spacing stands for the typical known crack saturation (higher loads). Microscopic investigations show that the fatigue damages only occur in the outer 90°-layers as matrix cracks and delaminations at the layer interface. The inner layers are damage-free.

The high damage ratios reached for LL1 and LL2 of TS1 and TS2 at comparatively low load cycle numbers (given under the specimen photo) lead to the classification into the HCF range. Due to the high damage ratios the damage parameters are not evaluated for the HCF range, as explained in Section 2.4. A first comparison concerning the influence of the layer thickness can be conducted for the fatigue damage limits. For TS1 and TS2 the limit is around LL5. The TS3 and TS4 show the limit rather between LL3 and LL4. A significant difference cannot be found for the tested layer thicknesses.

A clear contrast can be seen for the damage types. The test series with 0.5 mm layer thickness show larger crack spacing accompanying with large delaminations. For the thinner layers the ratio between the damage types is reversed with a small crack spacing and little delaminated areas. These first impressions shall be confirmed by the quantified damage parameters.

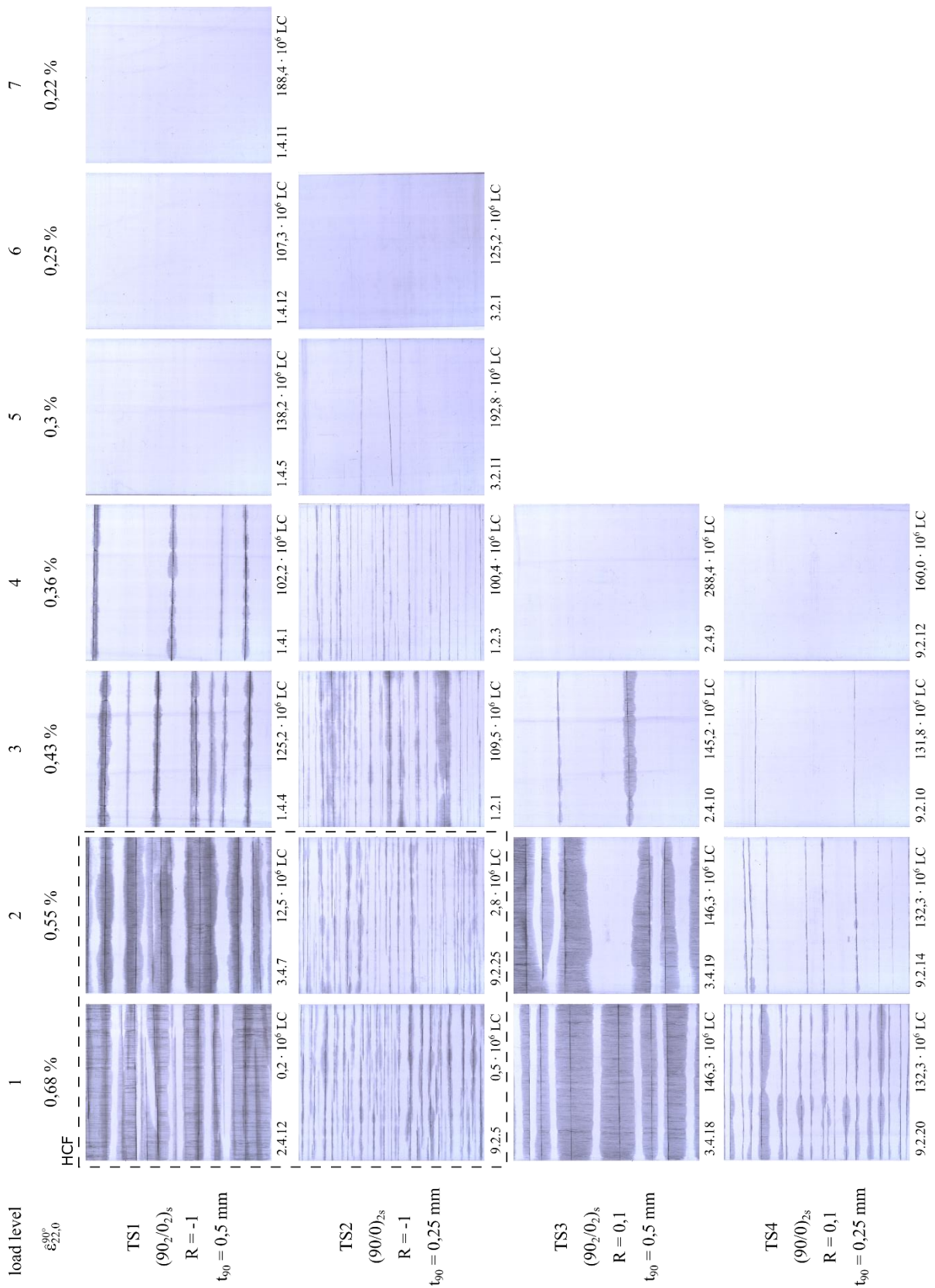


Figure 5: Overview of fatigue damage with one characteristic specimen for every test series and load level after the fatigue test.

4.2 Quantitative Damage Development

For every test series the degradation of the outer 90°-layer, the crack density and the delamination area ratio are determined and plotted over the load cycles in Figure 6. The curves of the specimens within a load level are averaged and the standard deviation is given as a grey area. A sudden change of the curves like for LL3 of TS1 is explained by a premature test ending of a specimen.

In general, all plots confirm the impression of increasing damage and degradation with rising loads from the damage overview in Figure 5.

For high loads, the crack density and delamination area ratio curves of all test series show a strong increase over the first $5 \cdot 10^6$ to $20 \cdot 10^6$ load cycles continuing with a slow and steady increase until 10^8 load cycles. The mechanical degradation of the 90°-layer fits to that.

The synchronous progress of the crack density and the delamination area ratio indicates the high tendency of this material towards delamination, which grow without delay with the occurrence of a crack.

For very low loads (LL6 and LL7) with no actual damage the flexural modulus rises. This contra intuitive behaviour is validated by the very accurate quasi-static testing of the specimens before and after the fatigue test. As for glass fibres no solidification is known, this phenomenon is expected to be reasoned in the polymer matrix. Polymers are known for solidification by an alignment of their long chain molecules, which might be seen in this graph.

The influence of the layer thickness concerning smaller crack spacing i.e. higher crack densities for 0.25 mm layers can be confirmed under alternating loads ($R = -1$) as well as swelling loads ($R = 0.1$).

In both cases the crack density approximately doubles for all load levels with cracks.

Under alternating loads the delamination area ratio is similar for both lay-ups. Taking the high crack density into account, it is clear that the delaminations per crack are higher for thick layers, as it is visible in the overview. Under swelling loads, the delamination area ratio is much higher for the thicker layers. It can be stated, that both damage types are strongly affected by the layer thickness. Therefore, the identified effects are investigated numerically.

4.3 Numerical Investigations

The effects found in the experimental results cannot be explained only by considering the different layer thicknesses. There are strong interactions between the damages, which need to be taken into account. For example, crack initiation stops at high crack densities (saturation) and delaminations do not grow together. To make the interactions visible, parameters for describing the tendency to the growth of the fatigue damage types need to be chosen. For crack growth normally parameters like the energy release rate or stress intensity factors are used. In the case of this study, the crack initiation is more relevant, because when an initiation takes place, in the majority a full-width crack develops, nearly unaffected by close damages. The initiation tendency is best represented by the maximum surface strain between two cracks. For the delamination growth, the stress intensity at the tip of the delamination is chosen. For heterogeneous materials like FRP normally the energy release rate is used for growth rates. For this study, not the released energy of crack growth, but the stress state around the crack tip should be represented. This is valid because the layers of the numerical model are designed as a homogeneous material. The resulting stress intensity factors K_I , K_{II} and K_{III} of the three crack opening modes are converted into an equivalent stress intensity developed by Richard and Sander [22] with the equation:

$$K_{EQ} = \frac{K_I}{2} + \frac{1}{2} \sqrt{K_I^2 + 5.336 K_{II}^2 + 4 K_{III}^2}. \quad (5)$$

The numerical calculations are conducted with the parametric model presented in Chapter 3.

The results of the parametric study are shown in Figure 7 with the maximum surface stress and the equivalent stress intensity in dependence of the crack density and the delamination area ratio. The simulation idealises irregular crack spacing and delamination lengths. It is conducted with three transverse cracks with equally growing delaminations. The stress intensity factors are calculated at the delamination tips of the centre crack.

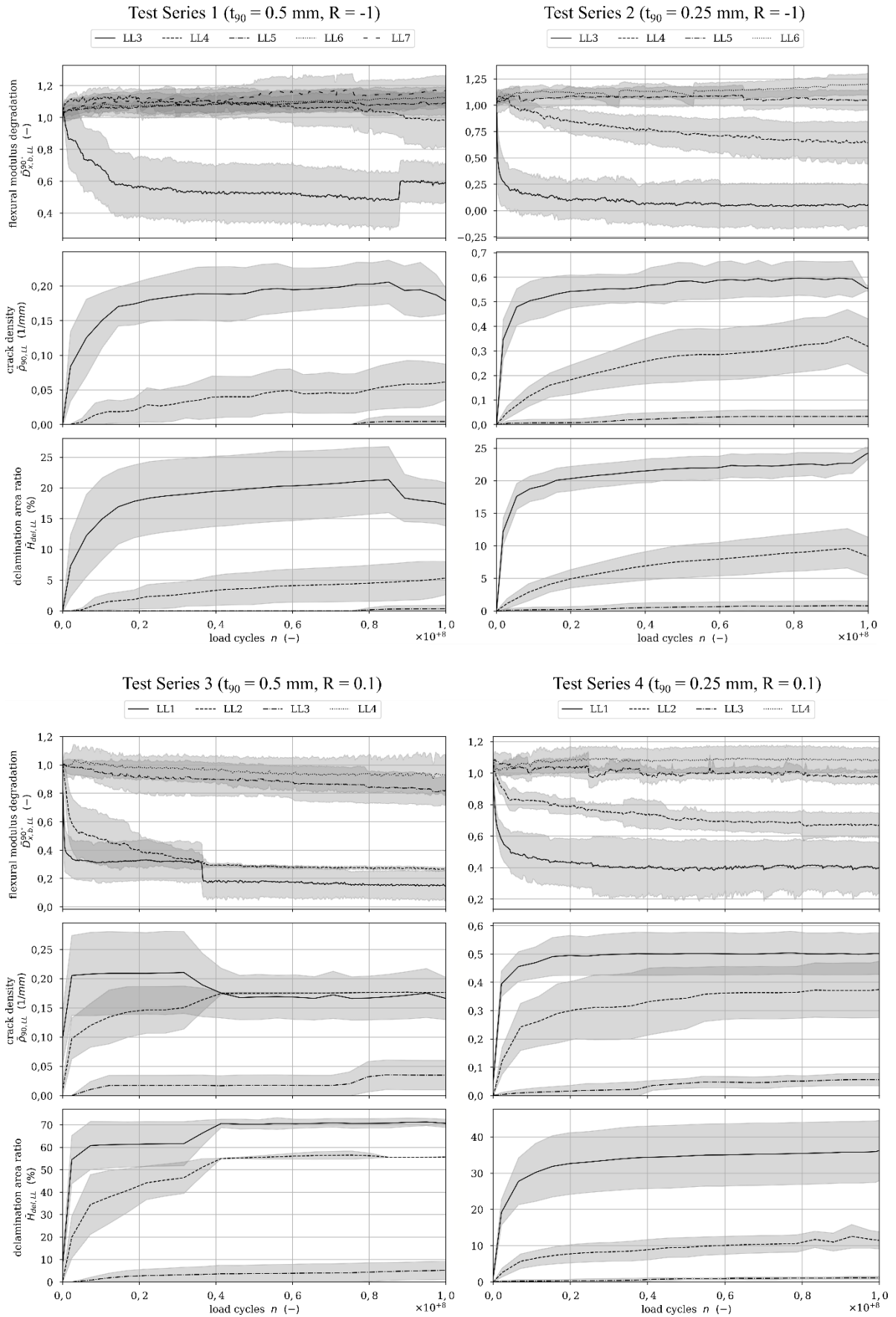


Figure 6: Development of the flexural modulus degradation, the crack density and the delamination area ratio, averaged over LL with standard deviation and smoothed for all TS.

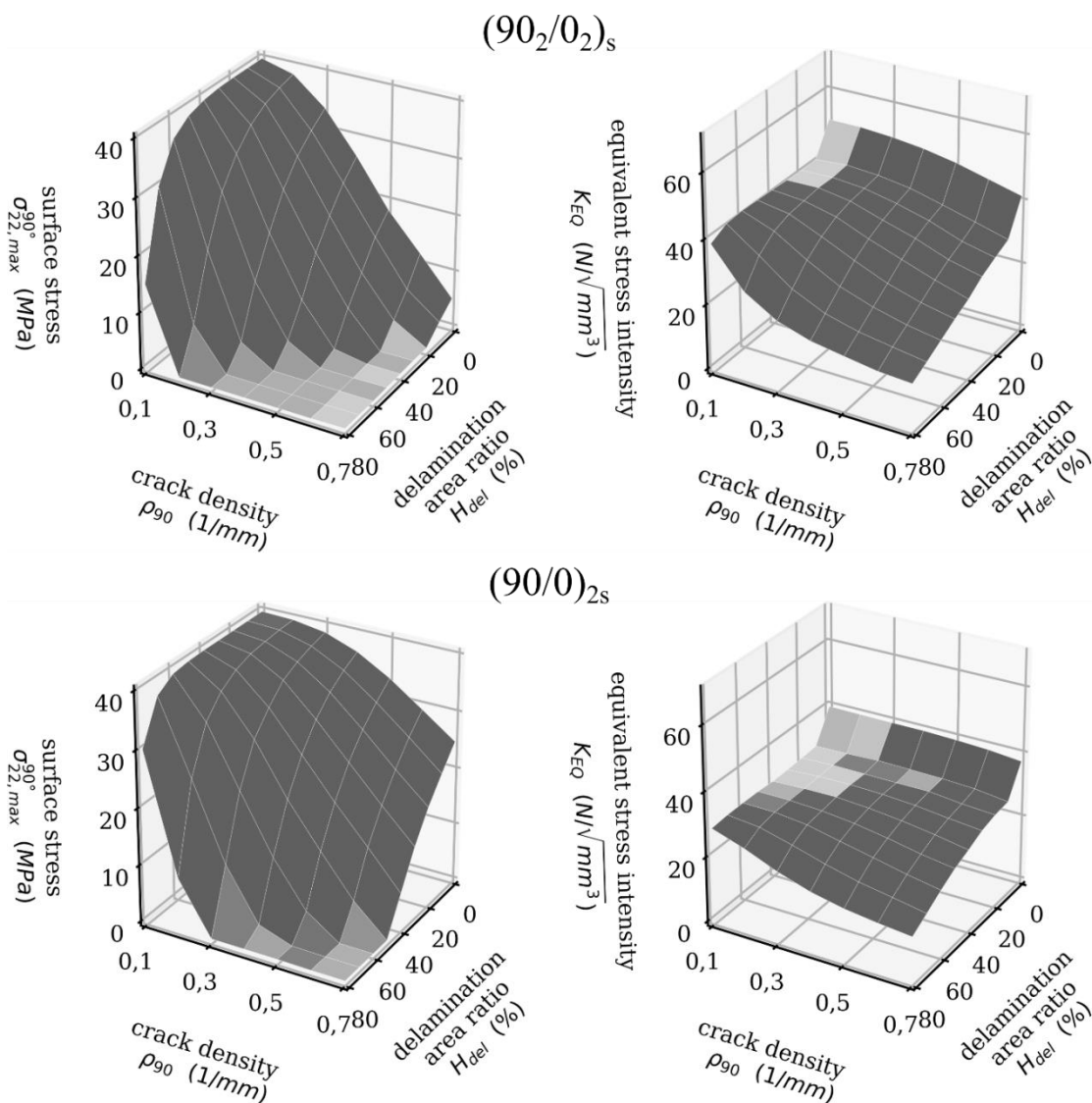


Figure 7: Influence of the crack density and the delaminations area ratio on the surface stress and equivalent stress intensity under four-point bending for load level 3.

Regarding crack initiation, the plots generally show decreasing surface stresses with the growth of both damage types. As the damages grow, a supposed transverse crack initiation limit is reached at some point, defined by the ratio between the two damage types. Reaching this limit is equivalent to the state of crack saturation.

Comparing the plots for both laminates, it is obvious that the surface stress of the thinner layer starts falling at higher damage ratios than for the thicker layers. This means cracks initiate at thin layers up to higher fatigue damage and therefore the high crack densities found in the experimental results can be reached.

The equivalent stress intensity, indicating the tendency towards delamination growth, behaves similarly. The plots show a strong increase at a delamination area ratio of $H_{del} = 0\%$. This is explained by the stress concentration in the vicinity of the transverse crack tip. For small and in case of thin layers also medium fatigue damage ratios, a plateau is visible. At this plateau a constant delamination growth is assumed, before the stress intensity falls with increasing damage, until a delamination growth limit is reached. On one hand the plateau for thick layers starts falling at lower damages, on the other hand its plane is higher. This means, the delamination growth for thicker layers is stronger without the influence of close damages, but the influence range is higher and the delamination growth stops at larger undamaged distances.

5. CONCLUSIONS

Extensive fatigue testing with 77 specimens tested up to 10^8 load cycles is conducted on an enhanced specialised VHCF-test rig. The results are verified by complimentary quasi-static tests and fatigue test evaluations. The fatigue evaluations include the mostly rare determination of quantitative damage parameters and their development over the fatigue load cycles.

Knowledge of basic effects like the higher crack density for thinner layers and stronger delaminations for thicker layers, which were known under tension load in the VHCF region (Hosoi et al. [14, 15]), can now be extended to four-point bending for alternating and swelling loads.

The effects are investigated in detail by a parametric fatigue damage simulation. Based on 3D-plots the strong interaction between existing damages and the influence of the layer thickness on the crack initiation and delamination growth are shown.

Acknowledgements

The authors gratefully acknowledge the financial support of the German Research Foundation (DFG) within the project "Fatigue and fatigue limits in the VHFC regime of thin fibre-reinforced polymer laminates" under grant agreement HO2122/28-1.

REFERENCES

- [1] J. F. Mandell and D. D. Samborsky, "DOE/MSU Composite Material Fatigue Database: Test Methods, Materials and Analysis," *Contractor Report SAND97-3002 Montana State University*, 1997.
- [2] J. C. Marin, A. Barroso, F. Paris and J. Canas, "Study of Fatigue Damage in Wind Turbine Blades," *Engineering Failure Analysis*, vol. 16, no. 2, p. 565–668, 2009.
- [3] C. Bathias, "An Engineering Point of View about Fatigue of Polymer Matrix Composite Materials," *International Journal of Fatigue*, vol. 28, p. 1094–1099, 2006.
- [4] P. Shabani, F. Taheri-Behrooz, S. S. Samareh-Mousavi and M. M. Shokrieh, "Very High Cycle and Gigacycle Fatigue of Fiber-Reinforced Composites: A Review on Experimental Approaches and Fatigue Damage Mechanisms," *Progress in Materials*, vol. 118:100762, 2021.
- [5] M. Bartelt, P. Horst and S. Heimbs, "Effects of an Enhanced Fibre-Matrix-Adhesion on the Fatigue Behaviour of Composite Materials under VHCF," *CEAS-Journal*, 2023.
- [6] R. Amacher, J. Cugnoni, J. Botsis, L. Sorensen, W. Smith and C. Dransfeld, "Thin Ply Composites: Experimental Characterization and Modeling of Size-Effects," *Composites Science and Technology*, pp. 121-132, 2014.
- [7] S. Sihn, R. Y. Kim, K. Kawabe and S. W. Tsai, "Experimental Studies of Thin-Ply Laminated Composites," *Composites Science and Technology*, pp. 996-1008, 2007.
- [8] A. Parvizi, K. W. Garrett and J. E. Bailey, "Constrained Cracking in Glass Fibre-Reinforced Epoxy Cross-Ply Laminates," *Journal of Materials Science*, pp. 195-201, 1978.
- [9] A. Hannig, Static and Fatigue Transverse Crack Initiation in Thin-Ply Fibre Reinforced Composites, PhD thesis: Technische Universität Braunschweig, Institut für Flugzeugbau und Leichtbau, 2018.
- [10] E. Boniface and S. Ogin, "Application of the Paris Equation to the Fatigue Growth of Transverse Ply Cracks," *Journal of Composite Materials*, vol. 23, pp. 735-752, 1989.
- [11] L. Boniface, P. A. Smith, S. L. Ogin and M. G. Bader, "Observations on Transverse Ply Crack Growth in a (0/90)₂s CFRP Laminate under Monotonic and Cyclic Loading," *6th International Conference on Composite Materials*, 1987.
- [12] S. L. Ogin and P. A. Smith, "Fast Fracture and Fatigue Growth of Transverse Ply Cracks in Composite Laminates," *Scripta metallurgica*, pp. 779-784, 1985.

- [13] L. Boniface, S. L. Ogin and P. A. Smith, "Strain Energy Release Rates and the Fatigue Growth of Matrix Cracks in Model Arrays in Composite Laminates," *Proceedings of the Royal Society of London. Series A: Mathematical and Physical Sciences*, pp. 427-444, 1991.
- [14] A. Hosoi and H. Kawada, "Fatigue Life Prediction for Transverse Crack Initiation of CFRP Cross-Ply and Quasi-Isotropic Laminates," *MDPI materials open access Journals*, 2018.
- [15] K. Kurihara, A. Hosoi, N. Sato and H. Kawada, "Effect of Ply Thickness on Transverse Crack Initiation in CFRP Cross-Ply Laminates under Fatigue Loading," *Transactions of the Japan Society of Mechanical Engineers, Part A*, vol. 79, no. 799, pp. 249-265, 2013.
- [16] T. J. Adam and P. Horst, "Very High Cycle Fatigue of Fibre-Reinforced Composites: An Alternative Experimental Approach," *Proceedings of the 19th Int. Conference on Composite Materials, ICCM19, Montreal*, pp. 5012-5021, 2013.
- [17] T. J. Adam and P. Horst, "Experimental Investigation of the Very High Cycle Fatigue of GFRP [90/0]s Cross Ply Specimens subjected to High-Frequency Four-Point Bending," *Composites Science and Technology*, vol. 101, pp. 62-70, 2014.
- [18] T. J. Adam and P. Horst, "Fatigue Damage and Fatigue Limits of a GFRP Angle-Ply Laminate," *International Journal of Fatigue*, 2017.
- [19] T. J. Adam, Ermüdungsverhalten faserverstärkter Kunststoffe im Very High Cycle Fatigue-Bereich, Braunschweig: TU Braunschweig - Niedersächsisches Forschungszentrum für Luftfahrt, 2016.
- [20] X. Chen, Fabrication and Experimental Material Characterization of RIM135/SE2020 (600Tex), Institut für Flugzeugbau und Leichtbau, TU Braunschweig, 2019.
- [21] H. A. Richard and M. Sander, Grundlagen der Bruchmechanik, Wiesbaden: Vieweg+Teubner, 2009.